

Article

Mechanical Property Characterization of Architectural Coated Woven Fabrics Subjected to Freeze–Thaw Cycles

Hastia Asadi ^{1,*} , Joerg Uhlemann ¹ , Natalie Stranghoener ¹  and Mathias Ulbricht ² 

¹ Institute for Metal and Lightweight Structures, Faculty of Engineering, University of Duisburg-Essen, Universitätsstr. 15, 45141 Essen, Germany; joerg.uhlemann@uni-due.de (J.U.); natalie.stranghoener@uni-due.de (N.S.)

² Lehrstuhl für Technische Chemie II, Faculty of Chemistry, University of Duisburg-Essen, Universitätsstr. 7, 45117 Essen, Germany; mathias.ulbricht@uni-due.de

* Correspondence: hastia.asadi@gmail.com

Abstract: This paper presents experimental investigations into the freeze–thaw response of two common architectural coated woven fabrics. Strip specimens for the tensile tests were exposed to $-20\text{ }^{\circ}\text{C}$ for three hours followed by three hours of thaw at ambient temperatures. This was repeated for a maximum of 100 cycles. Afterwards, the residual tensile strength was measured and compared to results achieved for test specimens without prior freeze–thaw cycles. Maximum mean tensile strength reductions of approximately 21% (warp direction) and 19% (weft direction) for probed polytetrafluoroethylene (PTFE)-coated woven glass fiber fabrics were identified, while no remarkable tensile strength deterioration rate was observed for the investigated polyvinyl chloride-coated woven polyethylene terephthalate materials. Overall, the results indicate that freeze–thaw cycles can have a significant deteriorating impact on the mechanical properties of glass-PTFE fabrics.

Keywords: artificial weathering; freeze–thaw condition; uniaxial tensile strength; secant modulus; strength modification factor



Citation: Asadi, H.; Uhlemann, J.; Stranghoener, N.; Ulbricht, M. Mechanical Property Characterization of Architectural Coated Woven Fabrics Subjected to Freeze–Thaw Cycles. *Textiles* **2024**, *4*, 26–39. <https://doi.org/10.3390/textiles4010003>

Academic Editor: Damien Soulat

Received: 2 November 2023

Revised: 2 January 2024

Accepted: 5 January 2024

Published: 11 January 2024



Copyright: © 2024 by the authors. Licensee MDPI, Basel, Switzerland. This article is an open access article distributed under the terms and conditions of the Creative Commons Attribution (CC BY) license (<https://creativecommons.org/licenses/by/4.0/>).

1. Introduction

Architectural coated fabrics as exterior building materials are exposed to destructive environmental impacts and can degrade over time. Weathering factors include solar radiation, moisture (pure water, saltwater, and acid rains), heat, oxygen and ozone, air pollution, biological factors, soiling, and mechanical stressors such as hail [1]. The acceptance of architectural coated fabrics for outdoor applications depends upon their exposed surface weatherability (both appearance and performance weathering resistance). One of the weathering stressors is water. It can be in the form of air humidity, rain, snow, hail, dew, and frost. Water can change the material properties by either chemical reactions such as hydrolysis or mechanical stress arising from swelling–deswelling sequences due to water content fluctuation or freeze–thaw cycles [2]. In fact, the effect of sudden or seasonal freeze–thaw cycling is of vital importance for membrane material durability. This active environmental stressor might influence the mechanical performance as well as mechanisms of fracture and failure by developing microcracks arising from compressive and tensile stresses. Cracking might occur in coating surfaces and fabric filaments. Water can seep through the thickness (out-of-plane watering, see Figure 1) and the length (in-plane watering) of coated woven fabrics. Probable mechanisms of out-of-plane water seepage are shown schematically in Figure 2. When water permeates the fabric, initially, it fills smaller capillaries, which are the original voids or cracks. Larger capillaries experience slower water penetration due to lower capillary pressure. However, the water retained within these larger capillaries serves as an additional reservoir for the smaller capillaries. There are also additional liquid reservoirs present at the intersection points of yarns. The presence of pinholes on the surfaces of both polyvinyl chloride-coated woven polyethylene

terephthalate (PET-PVC) and glass-PTFE materials (see Figure 2) confirms the potential for water to seep into fabric yarns. Out-of-plane water penetration is also induced by aging cracks. Over time, aging cracks develop, leading to delamination and a reduction in the protective coating's performance.

Water-induced degradation of fabrics by chemical reaction mechanisms was already investigated by Ansell [3] and Asadi et al. [4] on PET-PVC fabrics, and by Asadi et al. [4,5] Ansell et al. [6], and Toyoda et al. [7] on glass-PTFE fiber fabrics. Studies on PET-PVC materials proved that pure water at a temperature below glass transition of PET yarns ($T_g = 67\text{--}80\text{ }^\circ\text{C}$) causes no tensile strength deterioration [8], while above glass transition temperature, water leads to a reduction in the tensile strength due to bond cleavage in PET macromolecules and a reduction in polymer's crystallinity [6]. Ducoulombier et al. [9] surveyed the impact of acidic (to mimic acid rains) and basic media (to mimic water in contact with concrete surfaces) on two weaving patterns of PET-PVC fabrics (loose and tight weaving patterns) by an accelerated hydrolytic aging test at $70\text{ }^\circ\text{C}$. The acid solution was mimicking the rain composition, 0.3 mol/L of H_2SO_4 , $\text{pH} = 0.5$, for 35 days, while the basic medium was based on NaOH with $\text{pH} = 13.5$ for 32 days. They finally reported that the aging in acidic medium has no significant impact on the tensile strength, while the basic medium results in huge degradation effects.

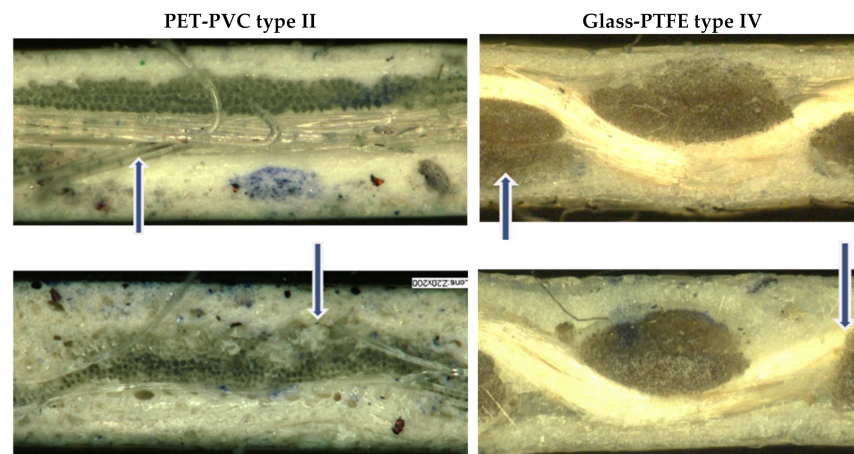


Figure 1. Ink penetration through the coating (blue pigments) after six days in ink-bath, cross-section view; blue arrow: water penetration direction [5].

All investigations related to the watering of glass-PTFE provide evidence of a considerable loss of tensile strength. The water contact with glass fibers of glass-PTFE composite, owing to some local defects in the final coating such as pinholes (see Figure 1) or incomplete coverage of glass fiber coating [9], is inevitable and independent from the water exposure duration, i.e., extended contact with water revealed only minimal additional detrimental effects [5]. Furthermore, glass-fiber is sensitive to moisture by static fatigue [10,11]. The combination of hydration, hydrolysis, and ion exchange [12] might be critical for glass fibers in contact with humidity because the chemical structure changes, i.e., bonds are cleaved. In the past, the impact of freeze–thaw has been surveyed generally on fiber-reinforced plastic but not specifically on PET-PVC and glass-PTFE materials. The freeze–thaw exposure causes microcracks on matrix, fibers as well as the fiber–polymer interface [13], which might change the fracture–failure mechanisms in loading conditions. These microcracks increase moisture penetration into the composite structures as well [14]. Cormier and Joncas [15] compared the results of freeze–thaw cycles on various composites and inferred that the tensile strength usually but not always was reduced. By increasing the range of temperature variation in freeze–thaw cycles, it was also observed that the ultimate tensile strength and modulus of elasticity of the composites diminish [16].

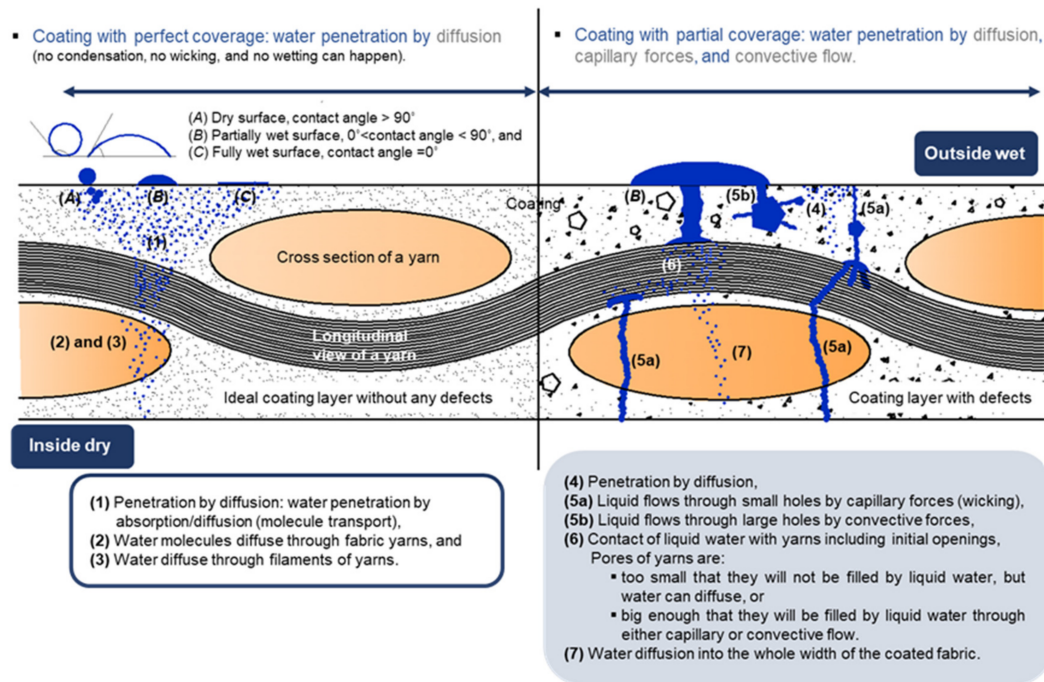


Figure 2. Different mechanisms of out-of-plane water penetration into coated fabrics.

Within this contribution, results of investigations into the freeze–thaw impacts on the mechanical properties, i.e., tensile strength and global stress–strain behavior of two common architectural fabrics, PET-PVC and glass-PTFE materials, are presented. The need to take into account the observed decrease in tensile strength in the design of tension fabric structures is acknowledged, and the strength modification factors associated with humidity effects, based on prCEN/TS 19102 [17], are proposed.

2. Materials and Methods

2.1. Materials

In this experimental study, membrane materials of PET-PVC types I and II and glass-PTFE types III and IV based on the type classification of prCEN/TS 19102 were used. Their main features are summarized in Table 1. Four batches of glass-PTFE type IV were employed. Both the PET-PVC and glass-PTFE materials were sourced from the same manufacturer, a prominent German producer whose products are widely utilized in tensioned membrane structures.

Table 1. Specifications of the investigated materials.

Sample ¹	Yarn	Total Weight ² [g/m ²]	Thickness ³ [mm]	Weave	Yarn Density ⁴ [dtex] Warp/fill	Yarn Count ⁵ [cm ⁻¹] Warp/Fill	Main Coating	Top Coating	Primer
PET-PVC type I	PET yarn	800	0.50	Plain 1/1	1100/1100	5.0/5.0	PVC	Acrylic polymer	-
PET-PVC type II	Low wick PET yarn	920	0.494	Planama 2/2	1100/1100	11.3/12.4		Polyvinylidene fluoride (PVDF)	TiO ₂
Glass-PTFE type III	E-glass fiber	1153	0.66	Plain 1/1	2040/2040	11/13	PTFE	-	-
Glass-PTFE type IV		1641	0.94		4080/4080	8/10		Fluorinated ethylene propylene (FEP) polymer	-

¹ Type according to tensile strength of producers' datasheets; ² mean of all batches measured based on EN ISO 2286-2:2017-01 [18]; ³ mean of all batches measured based on EN ISO 2286-3:2017-01 [19]; ⁴ mass per unit length (0.1 g/km) taken from producers' datasheets; ⁵ mean of all batches, measured based on EN 1049-2:1994-02 [20].

2.2. Methods

Freeze–thaw tests were carried out based on ASTM D7792/D7792M-15 [21]. In adherence to this standard, before initiating the freeze–thaw cycling, the specimens underwent a 30-day immersion in distilled water at $23\text{ }^{\circ}\text{C} \pm 2\text{ K}$ (designated as zero freeze–thaw cycle specimens). Subsequently, following the 30-day moisture exposure, the samples underwent a cold chamber treatment consisting of at least 3 h of exposure to air at $-20\text{ }^{\circ}\text{C} \pm 2\text{ K}$, followed by 3 h of immersion in distilled water at $23\text{ }^{\circ}\text{C} \pm 2\text{ K}$. This cycle was iterated for up to 100 freeze–thaw cycles. The cold chamber, produced by Liebherr and depicted in Figure 3, is capable of maintaining a consistent temperature as required. However, due to manual cycling operations, the specimens were left in a frozen state during nights and weekends.



Figure 3. Left: cold chamber, top right: glass-PTFE surface after freeze cycle, and bottom right: thaw cycle.

Tensile tests were carried out immediately at the end of the last exposure cycle. Tensile strength results of zero freeze–thaw cycles can establish the baseline properties prior to freeze–thaw cycling.

The uniaxial tensile behavior of the material was measured by a uniaxial constant rate extension machine according to the strip test method of EN ISO 1421 [22]. Elongation was measured using traverse travel. For both warp and weft directions, a set of specimens, comprising three or five samples, was taken. The stiffness (E_{secant}) was defined as the slope of a connecting line between zero stress and 25% of the maximum mean stress of virgin material (working stress range) on the mean stress–strain curve, as illustrated in Figure 4. E_{secant} provides a good representation of the material model typically used in structural design and analyses [17].

Generally, the tensile stress–strain curves of coated woven fabrics exhibit three regions: the inter-fiber friction region related to the friction resistance of yarns and their filaments; the decrimping region related to yarns unbending in loading direction with simultaneous crimp increase in transverse yarns; and finally, the yarn-extension region when yarns themselves carry the applied tensile stresses [23]. The three mentioned regions are observable in PET-PVC materials. However, in the case of glass-PTFE fabrics, the inter-fiber friction region is potentially absent, likely attributed to the anti-abrasive effect of the coating layer

on the glass filaments [5], cf. Figure 4. The water absorption in each strip exposed to freeze–thaw cycles is determined using Equation (1):

$$W_a = \frac{W_w - W_d}{W_d} \times 100\% \quad (1)$$

where W_a is the water absorption, W_d is the initial weight of the sample in its dry state, and W_w is the final weight of the sample after undergoing freeze–thaw cycles. Mean values of W_d and W_w were derived from three or five strips of each type.

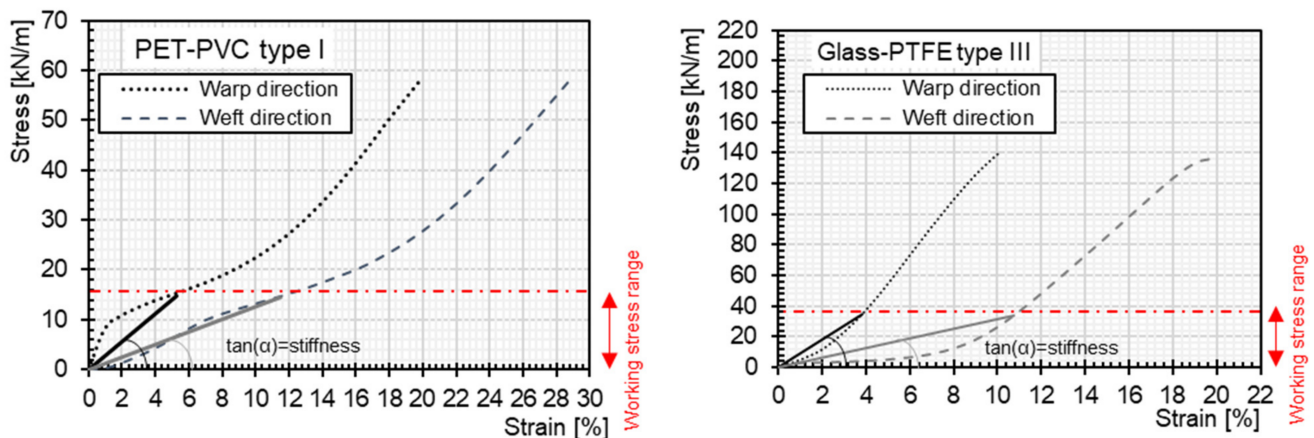


Figure 4. Connection line between the starting point and the 25% of the maximum stress (working stress range) utilized for stiffness calculation.

3. Results and Discussion

3.1. General

The possible loss of the mechanical properties by freeze–thaw exposure includes two mechanisms of moisture effect and extra stress arising from water volume alteration due to freezing cycles. As a matter of fact, the freeze–thaw cycles involve soaking strips in water (during either the initial 30 days or subsequent thaw processes) and freezing. The non-detrimental impact of distilled water alone on the tensile strength of PET-PVC materials [4] and PET yarns [8] has been validated before. Conversely, when in contact with glass-PTFE materials, distilled water leads to a deterioration in tensile strength [5].

3.2. PET-PVC Fabrics

3.2.1. Mean Stress–Strain Curves

Mean stress–strain curves derived from three or five specimens illustrate that the overall pattern, encompassing the three regions of inter-fiber friction, decrimping, and yarn extension, remains consistent after different freeze–thaw cycles. However, it is worth noting that the mean stress–strain curve for PET-PVC type I in the weft direction deviates slightly compared to the virgin state, as depicted in Figure 5. This is due to the fact that the standard deviations of the freeze–thaw state tests show higher values. Additionally, based on this figure, by increasing the number of freeze–thaw cycles for the investigated PET-PVC type II materials, the stress–strain curves remain almost unchanged except for the breaking points (maximum tensile strength).

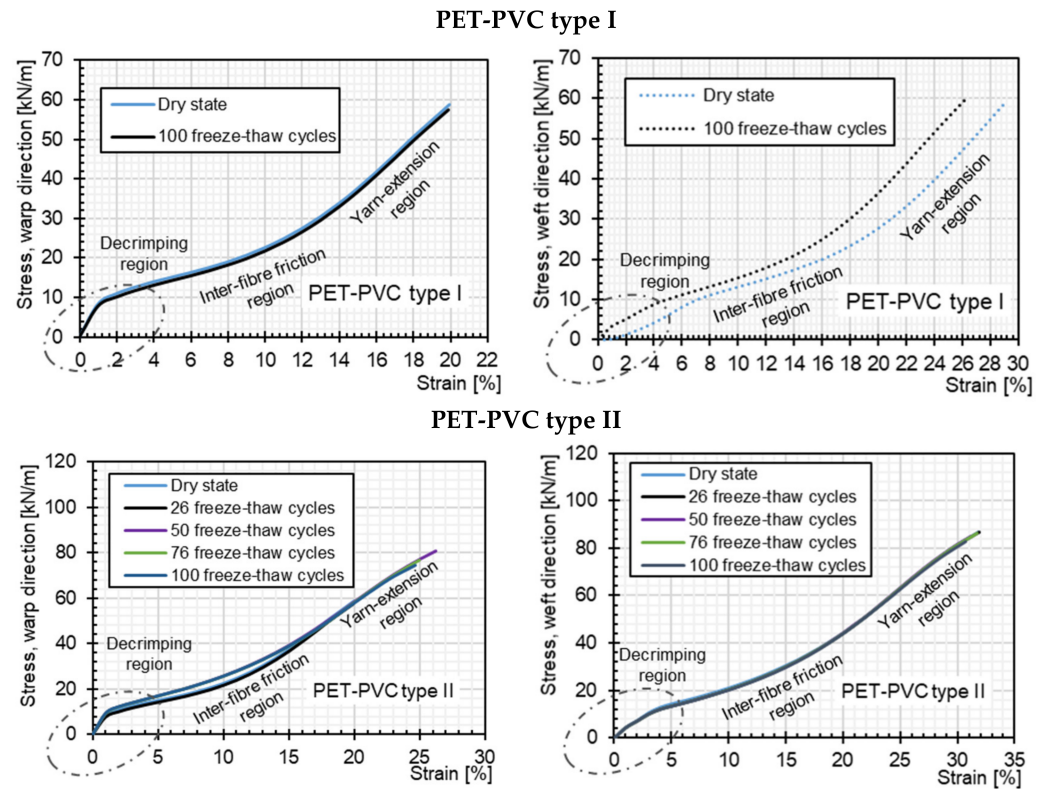


Figure 5. Mean stress–strain curves, virgin and freeze–thaw states, PET-PVC materials.

3.2.2. Weight Changes

Figure 6 illustrates the correlation between water absorption (refer to Equation (1)) and the number of freeze–thaw cycles for PET-PVC type II. According to the figure, water absorption rises from 0 to 50 cycles and subsequently reaches an almost constant (saturated) state for up to 100 cycles. The bar charts of Figure 5 display the average weight of PET-PVC type I and II at the initial dry state and after 100 freeze–thaw cycles. The water absorption for PET-PVC type I is about 5.0% for both principal directions, while for PET-PVC type II, it is 7.0% in warp and 7.6% in weft directions. This shows that the water absorption percentage of surveyed PET-PVC type II with low wick yarn systems is higher than that of PET-PVC type I without low wick systems. This contradicts the assumption that PET with low wicking properties absorbs less water. However, this difference might originate from the weaving pattern of PET-PVC type I with a yarn count of 5 warp/5 weft per cm and PET-PVC type II with a yarn count of 11.3 warp/12.4 weft per cm, cf. Table 1.

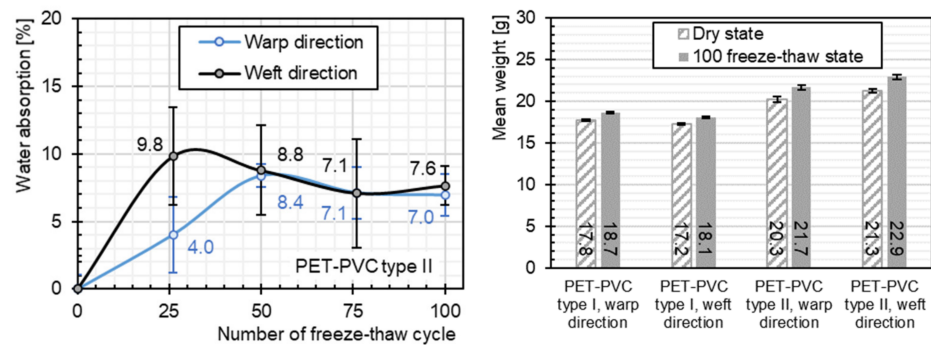


Figure 6. Changes of the mean weight, virgin (initial dry state) and freeze–thaw states, PET-PVC materials.

3.2.3. Stiffness Changes

The stationary relation between the mean value of E_{secant} (taken from three to five specimens) and the number of freeze–thaw cycles is illustrated in Figure 7. Bar charts of this figure also confirm the nonsignificant changes in Young’s modulus of freeze–thaw states compared to virgin dry ones.

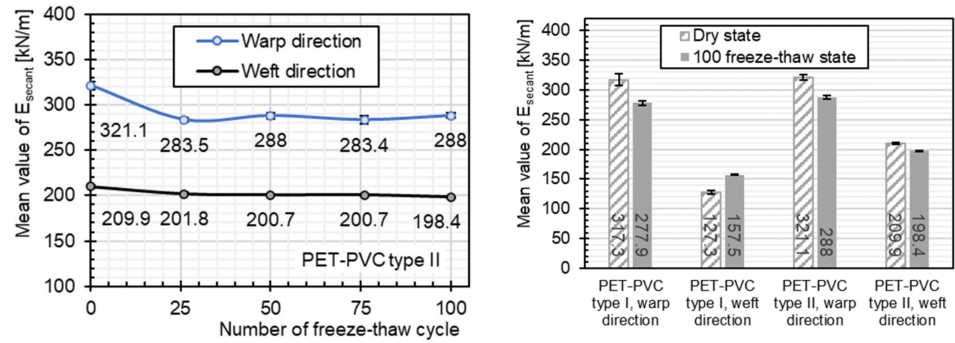


Figure 7. Relation between mean stiffness and number of freeze–thaw cycles, PET-PVC material.

3.2.4. Tensile Strength Changes

The residual tensile strength of PET-PVC type II for different numbers of freeze–thaw cycles is plotted in Figure 8. The two resulting curves for warp and weft directions approach almost steady states during an early stage of freeze–thaw experiments, while they reveal a decrease at the maximum number of 100 cycles. It is important to note that the most significant rate of deterioration in mean tensile strength, observed in PET-PVC type II in the warp direction, is associated with a considerable scattering of results around mean values. In conclusion, it can be summarized that freeze–thaw cycles have no substantial impact on the tensile strength of the materials under investigation. This suggests that PET is not only insensitive to water effects at temperatures below the glass transition temperature but also resilient to the additional stresses arising from water expansion and contraction during freeze–thaw cycles.

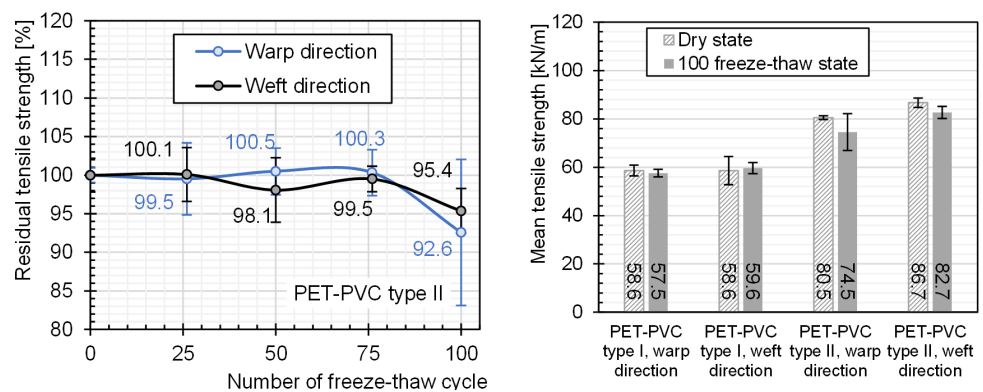


Figure 8. Tensile strength changes up to 100 freeze–thaw cycles, PET-PVC materials.

3.3. Glass-PTFE Fabrics

3.3.1. Mean Stress–Strain Curves

The results of the investigations into the mechanical performance of glass-PTFE fabrics under up to 100 freeze–thaw cycles have been achieved by uniaxial tensile testing. The mean stress–strain curves obtained from three to five specimens of glass-PTFE types III and IV, as illustrated in Figure 9, reveal an unaltered overall pattern in the decrimping and yarn-extension regions after exposure to freeze–thaw cycles. However, they exhibit lower breaking strength compared to the virgin (initial dry) strips.

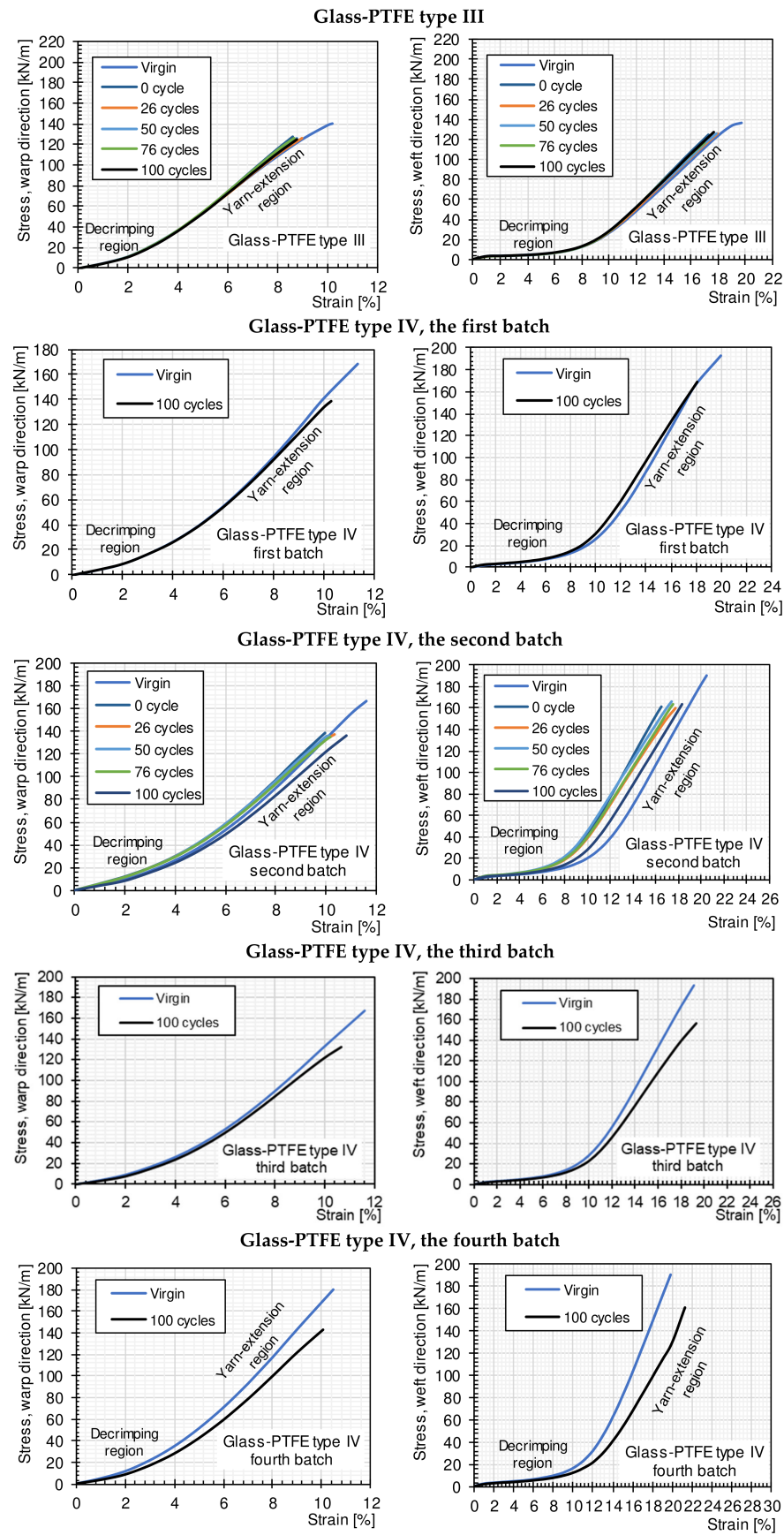


Figure 9. Mean stress–strain curves, virgin (initial dry state) and freeze–thaw states, glass-PTFE materials.

3.3.2. Weight Changes

Figure 10 provides a comparison of the relationship between the water absorption and number of freeze–thaw cycles for the investigated glass-PTFE materials. The rate of water absorption increases with an escalating number of freeze–thaw cycles. This trend is not as pronounced for specimens cut in the weft direction compared to those cut in the warp direction, observed in both surveyed glass-PTFE types III and IV.

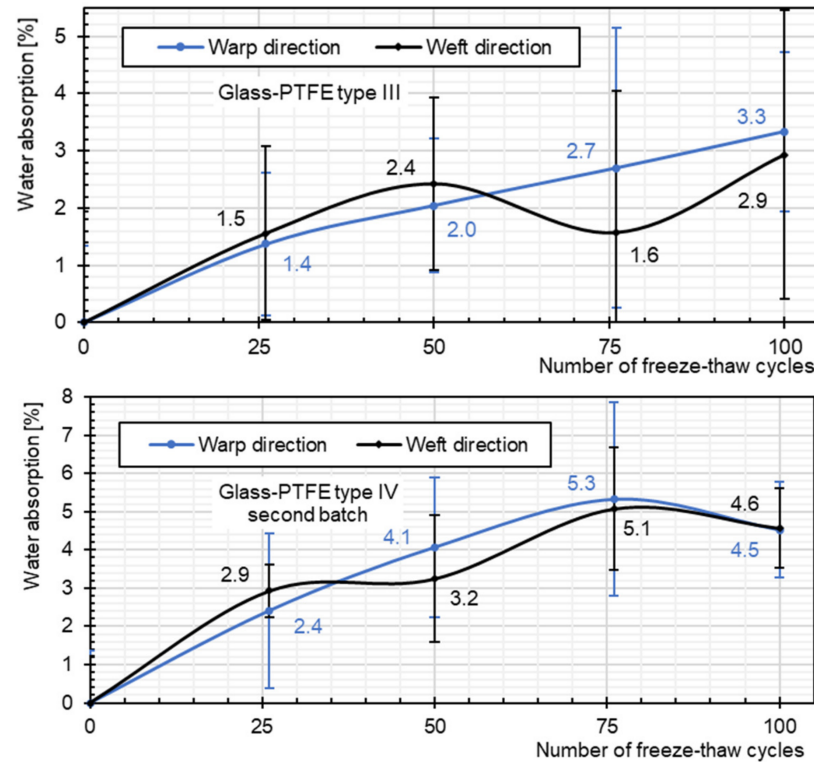


Figure 10. Comparison of relation between water absorption and number of freeze–thaw cycles, glass-PTFE materials.

3.3.3. Stiffness Changes

As already mentioned, glass-PTFE materials are sensitive to water attack solely. Therefore, zero freeze–thaw strips and initial dry strips were employed as two references in order to differentiate between the influence of only freeze–thaw cycles from the synergistic impact of water and freeze–thaw cycles, respectively. Here, the reference stiffness was determined as the slope of a connecting line between zero stress and 25% of the maximum mean stress of virgin and zero freeze–thaw cycle materials. Considering both indicators shown in Figure 11, E_{secant} does not change remarkably by increasing the number of freeze–thaw cycles. The mean value of E_{secant} after 100 freeze–thaw cycles compared to the virgin state (initial dry state), illustrated in Figure 12, confirms the nonsignificant changes in Young’s modulus of freeze–thaw states compared to virgin dry ones. Upon close examination of the nearly monotonic curves in Figure 11, it is hard to distinguish the influence of only freeze–thaw cycles from the combination of water and freeze–thaw cycles on the stiffness of investigated glass-PTFE types III and IV fabrics.

Stiffness progress under combination of water and freeze–thaw cycles (based on the slope of a connecting line between zero stress and 25% of the maximum mean stress of **virgin** material)

Stiffness progress under only freeze–thaw cycles (based on the slope of a connecting line between zero stress and 25% of the maximum mean stress of **zero** freeze–thaw cycle materials)

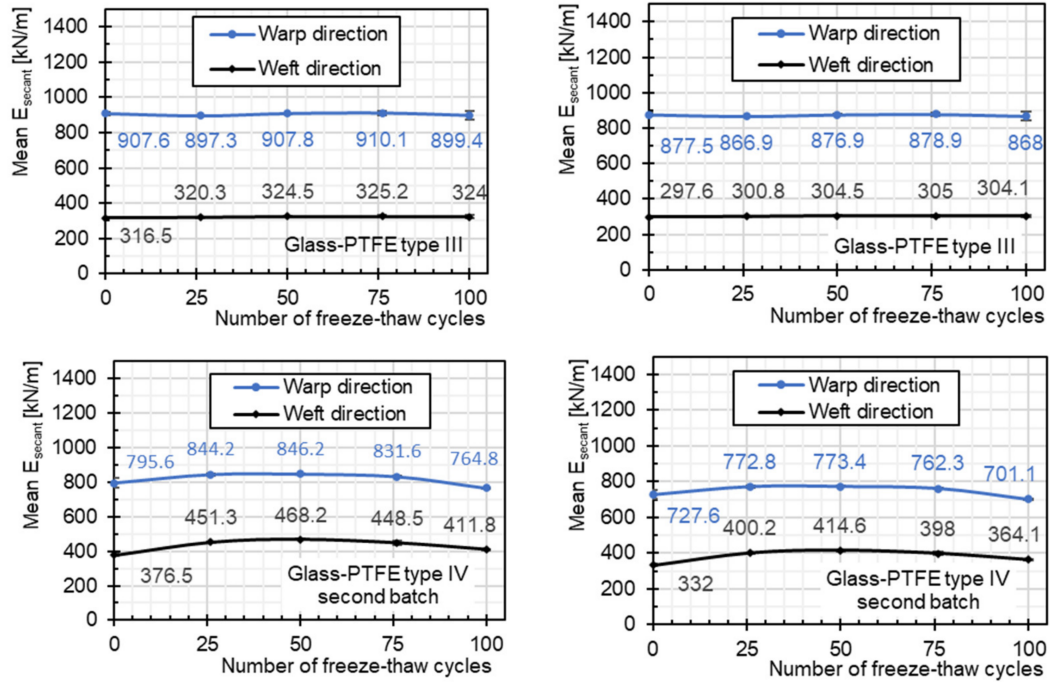


Figure 11. Relation between mean E_{secant} and number of freeze–thaw cycles, glass-PTFE materials (**left:** due to the combination of water and freeze–thaw cycles; **right:** due to only freeze–thaw cycles).

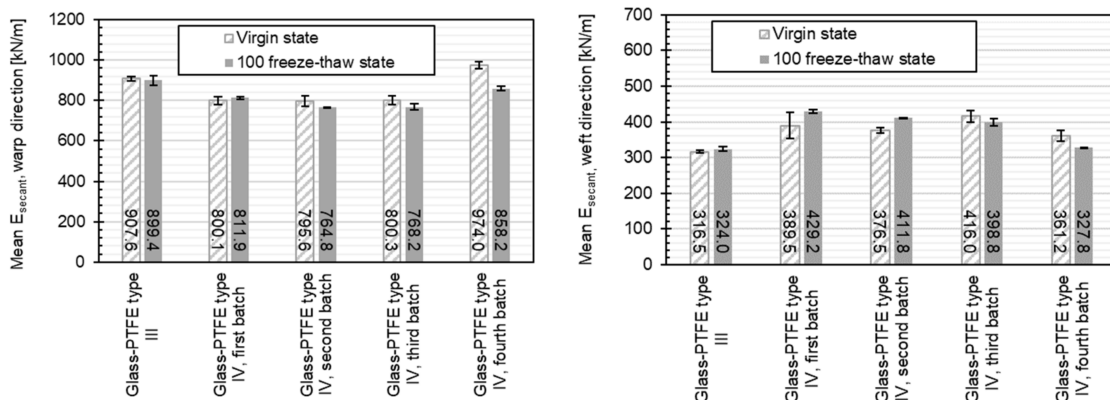


Figure 12. E_{secant} changes, virgin (initial dry state) and freeze–thaw states, glass-PTFE materials.

3.3.4. Tensile Strength Changes

Figure 13 illustrates the residual tensile strength of glass-PTFE types III and IV for various numbers of freeze–thaw cycles. In this figure, the combined impact of water and freeze–thaw cycles, using the initial dry strips as reference indicators, reveals a notable deterioration in tensile strength for both materials. When subjected to only freeze–thaw cycles, utilizing zero freeze–thaw strips as reference indicators, the tensile strength not only decreases insignificantly but, in some cases, increases. The highest rate of tensile strength reduction in the combined states of water exposure plus freeze–thaw cycles for

both investigated materials occurs at 26 cycles, after which the tensile strength almost reaches a plateau.

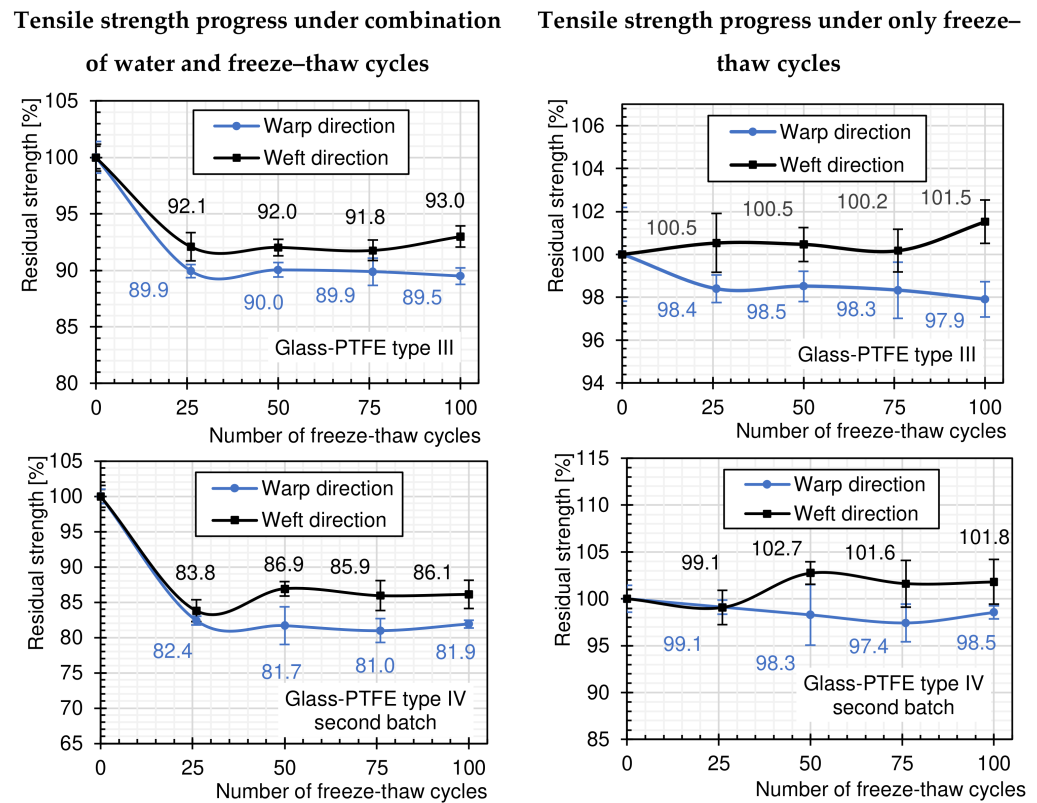


Figure 13. Relation between mean tensile strength and number of freeze-thaw cycles, glass-PTFE materials (**left:** due to combination of water and freeze-thaw cycles; **right:** due to only freeze-thaw cycles).

Moreover, the mean tensile strength (taken from three to five specimens) for all investigated glass-PTFE materials in virgin (initial dry state) and after 100 freeze-thaw states is depicted in Figure 14. The decreasing trend governs all investigated materials which clarifies the impact of water attack in combination with 100 freeze-thaw cycles. The highest percentage of tensile strength deterioration belongs to glass-PTFE type IV third batch (21.2% in warp and 18.8% in weft directions). The probed glass-PTFE materials type IV are more sensitive to this effect than type III. Asadi et al. [5] also provided evidence of the higher degree of sensitivity of glass-PTFE type IV (their materials and this contribution's materials were obtained from the same producer, but have different batch numbers) to water attack solely. They reported the highest tensile strength deterioration percentage of 17.2% in warp and 20.0% in weft directions. This comparison again outlines that the main decrease observed in the present study simply originates from the presence of water. The additional freeze-thaw cycles subsequent to watering have no significant impact on the tensile strength. As already mentioned, water can degrade glass through three mechanisms of hydration, hydrolysis, and ion exchange. According to Michalske and Bunker [12], these reactions are slow under normal ambient conditions. However, the rate of these reactions increases with elevated temperatures, and stress intensifies in extreme acid or basic environments. Additionally, when these three reactions occur simultaneously, each one influences the kinetics and mechanisms of the others.

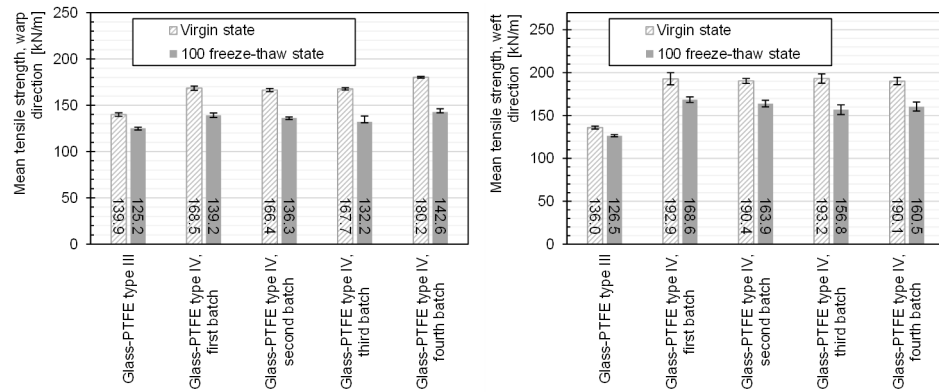


Figure 14. Tensile strength changes, virgin (initial dry state) and freeze–thaw states, glass-PTFE materials.

3.4. Strength Modification Factor Based on prCEN/TS 19102

The design process for tension fabric structures necessitates the consideration of alterations in material properties resulting from prolonged exposure to the environment [24]. In alignment with the harmonized perspective of the Ultimate Limit State, integrated into the design regulations for tension fabric structures, strength modification factors (k_i) are suggested in prCEN/TS 19102 [17] to characterize the tensile strength deterioration. While a comprehensive assessment of the modification factor induced by weathering and aging requires consideration of the synergistic effects of all environmental stressors, this contribution takes an initial step by proposing the strength modification factor k_{hum} . This factor aims to quantify the tensile strength deterioration resulting from freeze–thaw exposure, as outlined in Equation (2):

$$k_{hum} = \frac{f_{k,23,virgin}}{f_{k,23,freeze-thaw}} \tag{2}$$

where $f_{k,23,virgin}$ and $f_{k,23,freeze-thaw}$ express the 5% fractile values of short-term tensile strength at room temperature in virgin (initial dry state) and freeze–thaw states, respectively. It should be noted that among the two investigated materials, only glass-PTFE specimens indicate sensitivity to freeze–thaw exposures. The results of all freeze–thaw experiments for glass-PTFE materials are listed in the Supplementary Materials. Figure 15 depicts the scattered values of $k_{hum,5\%}$ at maximum 100 freeze–thaw cycles. The variability in results for both materials in both principal directions is substantial, with mean values for both clusters of glass-PTFE materials surpassing the recommended lower limit for the weathering-induced aging modification factor for glass-PTFE, denoted as $k_{age,min} = 1.1$ in accordance with prCEN/TS 19102. It is important to highlight that the suggested value in prCEN/TS 19102 is applicable to welding seams and accounts for the synergistic impact of all weathering stressors.

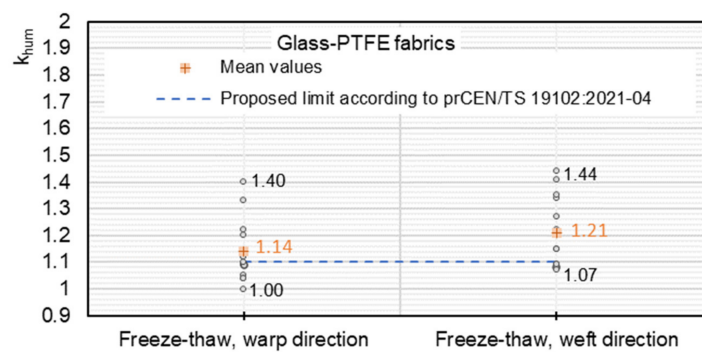


Figure 15. Scattered values of $k_{hum,5\%}$ for freeze–thaw up to 100 cycles.

4. Conclusions

The destructive effect of water as an aggressive environmental stressor through freeze–thaw cycles was studied experimentally, and the following conclusions were drawn:

1. Despite the potential for freeze–thaw cycles to induce internal stresses and to generate or extend microcracks, their presence, in this investigation, does not lead to significant additional tensile strength deterioration for investigated PET-PVC and glass-PTFE materials.
2. For PET-PVC, it can be summarized that freeze–thaw has no significant impact on the tensile strength of the investigated materials.
3. The simultaneity of moisture and freeze–thaw cycles have no significant influence on the tensile strength of glass-PTFE fabrics compared to moisture impact alone.
4. Upon exposure of glass-PTFE fabric to water, whether in the form of a chemical attack [5] or through freeze–thaw cycles, one can anticipate a degradation in tensile strength.
5. The highest percentage of tensile strength deterioration under the combined attack of water plus freeze–thaw cycles was 21.2% for probed glass-PTFE materials.
6. In both surveyed materials, the overall trend of the mean stress–strain curves does not reveal significant changes compared to their virgin states.

The reduction in tensile strength for both materials can be accounted for by employing strength modification factors. The average value of the modification factor k_{hum} , associated with up to 100 freeze–thaw cycles for glass-PTFE materials, surpasses the suggested lower limit for the weathering-induced aging modification factor specified in prCEN/TS 19102 for glass-PTFE, denoted as $k_{\text{age,min}} = 1.1$.

Supplementary Materials: The following supporting information can be downloaded at: <https://www.mdpi.com/article/10.3390/textiles4010003/s1>, Table S1: k_{hum} freeze–thaw cycles, glass-PTFE fabrics, warp direction; Table S2: k_{hum} freeze–thaw cycles, glass-PTFE fabrics, weft direction.

Author Contributions: Conceptualization, H.A. and J.U.; methodology, H.A., J.U., N.S. and M.U.; validation, J.U., N.S. and M.U.; formal analysis, H.A.; investigation, H.A., J.U., N.S. and M.U.; resources, N.S.; data curation, H.A. and J.U.; writing—original draft preparation, H.A.; writing—review and editing, H.A., J.U., M.U. and N.S.; visualization, H.A. and J.U.; supervision, J.U. and N.S.; project administration, N.S.; funding acquisition, N.S. All authors have read and agreed to the published version of the manuscript.

Funding: This research received no external funding. The Open Access Publication Fund of the University of Duisburg-Essen, Germany, supported the publication cost.

Data Availability Statement: Data are contained within the article or Supplementary Materials.

Acknowledgments: We acknowledge support by the Open Access Publication Fund of the University of Duisburg-Essen, Germany.

Conflicts of Interest: The authors declare no conflicts of interest.

References

1. Haillant, O. Accelerated weathering testing principles to estimate the service life of organic PV modules. *Sol. Energy Mater. Sol. Cells* **2011**, *95*, 1284–1292. [[CrossRef](#)]
2. Kockott, D. Natural and artificial weathering of polymers. *Polym. Degrad. Stab.* **1989**, *25*, 181–208. [[CrossRef](#)]
3. Ansell, M.P. The Degradative Effect of Boiling Water on Polyester Fibres in a PVC-Coated Fabric. *J. Ind. Text.* **1985**, *14*, 242–255. [[CrossRef](#)]
4. Asadi, H.; Uhlemann, J.; Stranghöner, N. Water infiltration impact on tensile strength and breaking strain of architectural fabrics. *Adv. Struct. Eng.* **2018**, *21*, 2605–2616. [[CrossRef](#)]
5. Asadi, H.; Uhlemann, J.; Stranghöner, N.; Ulbricht, M. Water Influence on the Uniaxial Tensile Behavior of Polytetrafluoroethylene-Coated Glass Fiber Fabric. *Materials* **2021**, *14*, 846. [[CrossRef](#)] [[PubMed](#)]
6. Ansell, M.P.; Hill, C.A.S.; Allgood, C. Architectural PTFE-Coated Glass Fabrics-Their Structure and Limitations. *Text. Res. J.* **1983**, *53*, 692–700. [[CrossRef](#)]

7. Toyoda, H.; Sakabe, H.; Itoh, T.; Konishi, T. Degradation of polytetrafluoroethylene-coated glass fiber fabrics by hot water treatment. *J. Fiber Sci.* **1995**, *51*, 282–286. [[CrossRef](#)] [[PubMed](#)]
8. Asadi, H.; Uhlemann, J.; Stranghöner, N.; Ulbricht, M. Artificial Weathering Mechanisms of Uncoated Structural Polyethylene Terephthalate Fabrics with Focus on Tensile Strength Degradation. *Materials* **2021**, *14*, 618. [[CrossRef](#)] [[PubMed](#)]
9. Ducoulombier, L.; Dakhli, Z.; Lafhaj, Z. Durability of textile facing materials for construction: Implementation of an accelerated aging test by hydrolysis. *J. Ind. Text.* **2014**, *45*, 1288–1307. [[CrossRef](#)]
10. Ishida, H.; Koenig, J.L. The reinforcement mechanism of fiber-glass reinforced plastics under wet conditions: A review. *Polym. Eng. Sci.* **1978**, *18*, 128–145. [[CrossRef](#)]
11. Griffith, A.A., VI. The phenomena of rupture and flow in solids. *Philos. Trans. R. Soc. A* **1921**, *221*, 582–593. [[CrossRef](#)]
12. Michalske, T.A.; Bunker, B.C. A Chemical Kinetics Model for Glass Fracture. *J. Am. Ceram. Soc.* **1993**, *76*, 2613–2618. [[CrossRef](#)]
13. Karbhari, V.M.; Rivera, J.; Dutta, P.K. Effect of Short-Term Freeze-Thaw Cycling on Composite Confined Concrete. *J. Compos. Constr.* **2000**, *4*, 191–197. [[CrossRef](#)]
14. Alkhader, M.; Zhai, X.; Chiang, F.P. Experimental investigation of the synergistic effects of moisture and freeze-thaw cycles on carbon fiber vinyl-ester composites. *J. Compos. Mater.* **2017**, *52*, 919–930. [[CrossRef](#)]
15. Cormier, L.; Joncas, S. Effects of Cold Temperature, Moisture and Freeze-Thaw Cycles on the Mechanical Properties of Uni-directional Glass Fiber-Epoxy Composites. In Proceedings of the 51st AIAA/ASME/ASCE/AHS/ASC Structures, Structural Dynamics, and Materials Conference, Orlando, FL, USA, 12–15 April 2010.
16. Ghasemi, A.R.; Moradi, M. Low thermal cycling effects on mechanical properties of laminated composite materials. *Mech. Mater.* **2016**, *96*, 126–137. [[CrossRef](#)]
17. *prCEN/TS 19102:2023-04*. Design of tensioned membrane structures (final draft, publication expected 2024).
18. *EN ISO 2286-2:2017-01*; Rubber- or Plastics-Coated Fabrics—Determination of Roll Characteristics—Part 2: Methods for Determination of Total Mass per Unit Area, Mass per Unit Area of Coating and Mass per Unit Area of Substrate. European Standard. CEN: Brussels, Belgium, 2017.
19. *EN ISO 2286-3:2017-01*; Rubber- or Plastics-Coated Fabrics—Determination of Roll Characteristics—Part 3: Method for Determination of Thickness. European Standard. CEN: Brussels, Belgium, 2017.
20. *EN 1049-2:1994-02*; Textiles—Woven Fabrics—Construction; Methods of Analysis—Part 2: Determination of Number of Threads per Unit Length. European Standard. CEN: Brussels, Belgium, 1994.
21. *ASTM D7792/D7792M-15*; Standard Practice for Freeze/Thaw Conditioning of Pultruded Fiber Reinforced Polymer (FRP) Composites Used in Structural Designs. ASTM International: West Conshohocken, PA, USA, 2015.
22. *EN ISO 1421:2016*; Rubber- or Plastics-Coated Fabrics—Determination of Tensile Strength and Elongation at Break. European Standard. CEN: Brussels, Belgium, 2016.
23. Colasante, G. Tensile Structures: Biaxial Testing and Constitutive Modelling of Coated Fabrics at Finite Strains. Ph.D. Thesis, Politecnico Di Milano, Milan, Italy, 2014. Available online: <https://www.politesi.polimi.it/handle/10589/97947> (accessed on 10 October 2017).
24. Asadi, H. Strength Deterioration of Architectural Fabrics under Single and Combined Artificial Weathering Impacts. Ph.D. Thesis, University of Duisburg-Essen, Essen, Germany, 2021. Available online: <https://nbn-resolving.org/urn:nbn:de:hbz:464-20220208-091716-1> (accessed on 8 February 2022).

Disclaimer/Publisher’s Note: The statements, opinions and data contained in all publications are solely those of the individual author(s) and contributor(s) and not of MDPI and/or the editor(s). MDPI and/or the editor(s) disclaim responsibility for any injury to people or property resulting from any ideas, methods, instructions or products referred to in the content.